

Published in final edited form as:

*Sci Transl Med.* 2014 March 26; 6(229): 229ra41. doi:10.1126/scitranslmed.3008326.

## Epigenetic reprogramming of HOXC10 in endocrine-resistant breast cancer

Thushangi N. Pathiraja<sup>1,2,3</sup>, Shweta Nayak<sup>4</sup>, Yuanxin Xi<sup>5</sup>, Shiming Jiang<sup>3,15</sup>, Jason P. Garee<sup>2,6</sup>, Dean P. Edwards<sup>7,13</sup>, Adrian V. Lee<sup>2,7</sup>, Jian Chen<sup>7</sup>, Martin J. Shea<sup>2</sup>, Richard J. Santen<sup>8</sup>, Frank Gannon<sup>11</sup>, Sara Kangaspeska<sup>11,14</sup>, Jaroslav Jelinek<sup>10</sup>, Jean-Pierre J. Issa<sup>10</sup>, Jennifer K. Richer<sup>11</sup>, Anthony Elias<sup>11</sup>, Marie McIlroy<sup>12</sup>, Leonie Young<sup>12</sup>, Nancy E. Davidson<sup>7</sup>, Rachel Schiff<sup>2</sup>, Wei Li<sup>5</sup>, and Steffi Oesterreich<sup>2,7</sup>

<sup>1</sup>Graduate Program in Translational Biology and Molecular Medicine, Baylor College of Medicine, Houston, TX 77030 <sup>2</sup>Lester and Sue Smith Breast Center, Baylor College of Medicine, Houston, TX 77030 <sup>4</sup>Magee Women's Hospital, Reproductive Endocrinology and Infertility, Pittsburgh, PA

<sup>3</sup>Current address: Genome Institute of Singapore, Singapore 138672

<sup>6</sup>Current address: Georgetown University, Washington, DC 20057

<sup>9</sup>EMBL, Heidelberg, Germany, Current address: QIMR Berghofer Medical Research Institute, Australia 4006 69117

<sup>14</sup>Current address: Institute for Molecular Medicine, Finland 00290

<sup>15</sup>Current address: UT MD Anderson Cancer Center 77030.

### Supplementary materials:

#### Material and Methods

#### Supplementary Figures

Fig S1: Characterization of C4-12 and LTED cells.

Fig S2: E2 response in MCF-7, MDA-MB-134VI, and HCC1395.

Fig S 3: ER ChIP LTED cells.

Fig S4: E2 regulation of classical ER target genes in LTED cells.

Fig S5: Loss of E2 response results in modest changes in EZH2 recruitment and trimethylation of H3K27 and H3K4 at HOXC10 proximal promoter region.

Fig S6: Increased growth upon HOXC10 knockdown is not generalizable to all breast cancer cell lines.

Fig S7: Loss of HOXC10 mediates tamoxifen resistance.

Fig S8: *In vivo* growth of HOXC10 knockdown clone sh-H2.

#### Supplementary Tables

Table S1: Differentially methylated (hyper and hypo) genes in C4-12 and LTED compared to MCF7

Table S2. Original data for graphs that show composite results

Table S3: Exact p-values for statistical analyses

Table S4: Significant GO terms for hypermethylated genes in C4-12 and LTED.

Table S5: List of q-PCR primers

Table S6: List of bisulfite sequencing primers

### Author contributions:

T.N.P, S.N, S.J, J.P.G, D.E, A.V.L, J.C, M.S, R.J.S, F.G, S.K, J.J, J-P.J.I, J.R, A.E, L.Y, N.E.D, R.S, W.L, S.O participated in design and/or interpretation of experiments or results, acquisition and/or analysis of data, and drafted and or revised the manuscript. R.J.S participated in design and/or interpretation of experiments or results, and drafted and or revised the manuscript. DE was primarily responsible for data in Fig 2E. AE was primarily responsible for the clinical trial and banking tissues. JC was primarily responsible for growth curve analyses. J.J., T.N.P, S.N were primarily responsible for DNA methylation analysis. SK was primarily responsible for the methylation pull-down concept and subsequent advice. WL and YX were primary responsible for bioinformatic analysis of methylation pull-down data. SN was primarily responsible for acquisition of human tumors and HOXC10 expression analysis. JKR, MM, and LY were primary responsible for advice on IHC and staining of human primary and metastatic tumors. MS and RS were primary responsible for the *in vivo* xenograft work. A.V.L, J.C, M.S, R.J.S, F.G, S.K, J.J, J.R, A.E, L.Y, S.O provided administrative, technical or supervisory support.

### Competing interests:

The authors declare that they have no competing interests.

### Materials and data availability:

The data from the MBD-PD array have been deposited into Gene Expression Omnibus data base repository under GSE39783.

15213 <sup>5</sup>Dan L Duncan Cancer Center, Baylor College of Medicine, Houston, TX 77030 <sup>7</sup>Women's Cancer Research Center, University of Pittsburgh Cancer Institute (UPCI) and Magee-Womens Research Institute, University of Pittsburgh Cancer Center, Pittsburgh, PA 15213 <sup>8</sup>University of Virginia Health Sciences Center, Charlottesville, VA 22903 <sup>10</sup>Temple University, Fels Institute, Philadelphia, PA 19140 <sup>11</sup>University of Colorado Anschutz Medical Campus, Department of Pathology and Department of Medicine, Denver, CO 80202 <sup>12</sup>Royal College of Surgeons of Ireland, Dublin 2, Ireland <sup>13</sup>Department of Molecular and Cellular Biology, and Pathology and Immunology, Baylor College of Medicine, Houston, TX 77030

## Abstract

Resistance to aromatase inhibitors (AIs) is a major clinical problem in the treatment of estrogen receptor positive breast cancer. In two breast cancer cell line models of AI resistance we identified widespread DNA hyper- and hypomethylation, with enrichment for promoter hypermethylation of developmental genes. For the homeobox gene HOXC10, methylation occurred in a CpG shore which overlapped with a functional ER binding site, causing repression of HOXC10 expression. Although short-term blockade of ER signaling caused relief of HOXC10 repression in both cell lines and breast tumors, it also resulted in concurrent recruitment of EZH2 and increased H3K27me3, ultimately transitioning to increased DNA methylation and silencing of HOXC10. Reduced HOXC10 in vitro and in xenografts resulted in decreased apoptosis and caused antiestrogen resistance. Supporting this, we used paired primary and metastatic breast cancer specimens to show that HOXC10 was reduced in tumors which recurred during AI treatment. We propose a model in which estrogen represses apoptotic and growth inhibitory genes such as HOXC10, contributing to tumor survival, whereas AIs induce these genes to cause apoptosis and therapeutic benefit, but long-term AI treatment results in permanent repression of these genes via methylation and confers resistance. Therapies aimed at inhibiting AI-induced histone and DNA methylation may be beneficial in blocking or delaying AI resistance.

## INTRODUCTION

Approximately 70% of breast tumors express estrogen receptor  $\alpha$  (ER), and patients with these tumors are candidates for endocrine therapy such as tamoxifen and aromatase inhibitors (AI). Despite the well documented benefits of endocrine therapy, not all patients with ER+ tumors initially respond to endocrine therapy ("de novo resistance"), and many ER+ tumors eventually become refractory to therapy ("acquired resistance") (1). AIs, which block the conversion of androgen to estrogen and thus lower systemic estrogen, have superior efficacy for the treatment of postmenopausal ER+ breast cancer compared to tamoxifen (2). Although a large body of literature has identified possible mechanisms of resistance to tamoxifen, less is known about the mechanisms of resistance to AIs (3).

A number of possible mechanisms for endocrine resistance have been described, such as the bidirectional crosstalk between steroid receptors and growth factor receptors (4). The targeting of mTORC1 with everolimus has recently shown great promise in the treatment of endocrine-resistant ER+ disease (5). Deregulation of estrogen signaling and altered

expression of coactivators and corepressors have been reported to be associated with endocrine resistance (6). This occurs as a consequence of genetic changes, such as amplification of AIB1 (7), ERBB2 (8), and more recently ESR1 mutations (9). However, there is increasing evidence implicating epigenetic mechanisms in the development of resistance. For example, resistance to tamoxifen has been associated with promoter hypermethylation and hypomethylation of a number of genes (10). In contrast, very few studies have focused on epigenetic changes in breast cancer cells resistant to estrogen deprivation (11).

We performed a genome-wide methylation screen using two independent long-term estrogen deprived cell lines derived from MCF-7, termed C4-12 and LTED. We identified genome-wide hyper- and hypomethylation with enrichment for developmental genes, including a number of homeobox genes. HOXC10, a gene repressed by estrogen in hormone-responsive MCF-7 cells, was repressed through epigenetic mechanisms after estrogen withdrawal. This epigenetic reprogramming included EZH2 recruitment, repressive histone marks, and subsequent DNA methylation. We propose a model whereby estrogen represses HOXC10 to promote tumor growth, whereas AI block estrogen action to induce HOXC10. HOXC10 apoptotic and growth-inhibitory functions may contribute to the therapeutic effect of AI, however, long-term estrogen deprivation leads to permanent epigenetic silencing of HOXC10, which counteracts the AI-mediated induction of these genes and contributes to acquired endocrine resistance.

## RESULTS

### DNA methylation frequently changes in breast cancer cells resistant to estrogen deprivation

C4-12 and LTED cells, two previously established MCF-7 sublines that are resistant to estrogen deprivation, were used for the studies (Fig 1A). C4-12 cells were previously shown to be ER-negative (12), while LTED cells maintain high levels of ER (13). Loss of ER in C4-12 is only partially due to methylation, as the majority of the ESR1 promoter is unmethylated (Fig S1A). These two cell line models are representative of clinical AI-resistant breast tumors, which can be ER+ or ER-. They are resistant to estrogen-deprivation; however, they have not undergone EMT, as expression of classical EMT markers (14) showed inconsistent changes (Fig S1B).

We performed a genome-wide methylation screen with a previously described assay (15), which uses affinity-based enrichment of methylated regions of DNA via a methylation binding domain (MBD). We detected a total of 267 and 301 hypermethylated genes in C4-12 and LTED, respectively, compared to MCF-7 (Table S1) (fold change cut-off >2). Hypomethylation was less frequently observed, with 82 and 97 hypomethylated genes in C4-12 and LTED, respectively. There was a highly significant overlap of hypermethylated ( $p = 6.1E^{-79}$ ) and hypomethylated genes ( $p = 2.4E^{-23}$ ) between C4-12 and LTED (Fig 1B), suggesting that there were many epigenetic modifications shared between these two independent models of resistance to estrogen deprivation.

Given the well-known effect of hypermethylation on gene silencing, we focused on hypermethylation events. DNA methylation peaks from the MBD-PD assay showed that the promoters of DOK5, BMP4, ZFP37 were hypermethylated in C4-12 and LTED by ~5 to ~10 fold (Fig 1C left panel). For all three genes, bisulfite sequencing confirmed the MBD-PD result, although the actual magnitude of methylation was somewhat variable (Fig 1C).

72 genes were commonly hypermethylated between C4-12 and LTED cells (Fig 1B). Gene Ontology analysis showed a marked enrichment of genes involved in developmental processes (Table S2). Given the increasingly recognized importance of HOX genes in tumorigenesis, we focused subsequent studies on HOXC10, which was highly methylated in both C4-12 and LTED cells.

### **Methylation of HOXC10 promoter is associated with transcriptional silencing**

The HOXC10 gene has a clearly defined CpG island spanning its proximal promoter and extending over the first exon (Fig 2A). The distal promoter region showed almost complete DNA methylation in both C4-12 and LTED, with no detectable methylation in MCF-7 (Fig 2B). This methylated region falls into the category of 'CpG island shore' methylation, an event that has been described for other cancer cells, as well as for stem cells (16, 17). There was also an increase in methylation of the exonic region, although the difference between MCF and the resistant cell lines was less striking. In contrast, the proximal promoter was unmethylated in MCF7, C4-12 and LTED cells.

Quantification of HOXC10 mRNA in MCF-7, C4-12, and LTED cells showed that methylation was associated with transcriptional silencing (top panel in Fig 2C; table S3). The decreased expression of HOXC10 in breast cancer cells resistant to estrogen deprivation was not unique to MCF-7, because it was also observed in resistant cell line models generated from MM361, ZR-75B, T47D, and BT474 breast cancer cells (bottom panel in Fig 2C; table S3). Treatment of C4-12, LTED and MCF-7 cells with the DNA methylation inhibitor 5' aza-deoxycytidine (DAC) and the histone deacetylase (HDAC) inhibitor Trichostatin A (TSA) showed that repression of HOXC10 was not only mediated by DNA methylation, but may also involve additional repressive histone modifications (Fig 2D; table S3). Treatment with TSA significantly induced HOXC10 expression in both C4-12 ( $p=0.025$ ) and LTED cells ( $p=0.0007$ ), but not in MCF-7 cells ( $p=0.279$ ).

We analyzed HOXC10 expression and methylation in a large number of breast cancer cell lines. Methylation at the 'CpG island shore' varied widely from 5 to 95%, whereas very little methylation was detected at the proximal promoter region (Fig 2E; table S3). HOXC10 methylation at the CpG island shore and the amount of transcript were inversely correlated ( $r = -0.61$ ,  $p = 0.001$ ), with a weaker association at the proximal promoter region ( $r = -0.36$ ,  $p = 0.034$ ). There was also an association between HOXC10 mRNA expression and ER status of the cell lines: the majority (76%) of the ER+ cell lines expressed HOXC10 above the average level, but only 28% of ER- cell lines expressed HOXC10 above the average level. Intriguingly, the two ER+ cell lines in which HOXC10 was hypermethylated (MDA-MB-134-VI and HCC-1395, indicated with arrows in Fig 2E) show decreased estrogen (E2) response compared to other ER+ cells (Fig S2), suggesting that there is an inverse correlation between HOXC10 methylation and ER levels, and also ER function.

## Estrogen regulates HOXC10 expression

The preferential expression of HOXC10 in ER+ cells (Fig 2E) indicated that regulation of HOXC10 expression might be under estrogen control. The HOXC10 promoter has 6 half estrogen response element (ERE) sites and 1 palindromic full ERE site, with only one mismatch compared to the consensus ERE (Fig 3A). The ERE maps to the CpG island shore which is hypermethylated in the C4-12 and LTED cells, as well as in many ER-negative cell lines. Chromatin immunoprecipitation (ChIP) assays revealed strong estrogen-induced ER recruitment to the ERE at the -1.6 kb region, and modest recruitment to the -0.1 kb region (Fig 3B; table S3). As a positive control, we used recruitment to pS2 ERE, and as a negative control we used the lack of ER recruitment to a non-functional ERE (NFERE) (18). Interestingly, ER was also recruited (albeit more weakly) to the HOXC10 promoter in LTED cells (Fig S3), suggesting that i) ER can be recruited to a methylated region, and ii) ER recruitment is not sufficient for transcriptional activation.

To examine if ER recruitment resulted in estrogen regulation of HOXC10 gene expression, we treated MCF-7 and LTED with estradiol (E2) and the anti-estrogen ICI 182,780 (ICI). E2 caused repression of HOXC10 mRNA expression, which was blocked by ICI (Fig 3C; table S3). As expected, E2 and ICI did not change the minimal HOXC10 expression in LTED cells. Of note, LTED cells retain the ability of estrogen to regulate many other classical E2-regulated genes (Fig S4), consistent with a previous report (19). As expected, these genes were not identified in the LTED MBD-PD array as being significantly methylated, using cut-offs of  $p < 10^{-5}$  and fold change  $>2$  in the MAT analysis (Table S1).

To determine whether estrogen regulation of HOXC10 was also observed in clinical breast tumors, we measured HOXC10 levels by immunohistochemistry (IHC) in 30 matched pre and post-treatment samples (15 pairs) from women with early breast cancer who received 4 months of neoadjuvant exemestane treatment (Fig 3D). Baseline expression levels varied widely; however, there was a significant increase in total HOXC10 after short-term treatment with AI, as one would expect for an estrogen-repressed gene (paired t-test,  $p=0.02$ ). This induction was more pronounced for cytoplasmic HOXC10 ( $p=0.003$ ) compared to nuclear HOXC10 (n.s.) (Fig 3E).

Because histone methylation is known to be critical for long-term repression of HOX genes during embryonic development (20), we determined whether estrogen regulation, or loss thereof, was associated with altered EZH2 recruitment to the HOXC10 promoter. E2 deprivation (veh) of MCF-7 cells resulted in EZH2 recruitment and trimethylation of H3K27 at the distal HOXC10 promoter region (Figs 3F and 3G, left panel; table S3), but not at the proximal promoter (Fig S5). A similar increase in EZH2 recruitment and H3K27me3 was observed when ER signaling was blocked with ICI (Fig 3F and 3G; table S3). A strong recruitment of EZH2 (Fig 3F; table S3) and H3K27me3 (Fig 3G; table S3) was also detected in C4-12 and LTED cells, with minor effects of EZH2 recruitment in the ER-negative MDA-MB-231 cells, which are de-novo resistant to estrogen. Because HOX genes show bivalent repressive H3K27me3 and active H3K4me marks during development (21, 22), we also studied methylation at H3K4 by ChIP and found strong recruitment in MCF-7 cells, which was decreased in C4-12 and LTED, and absent in the MDA-MB-231 cells (Fig 3H; table S3).

Collectively, these data suggest that short-term blockade of ER signaling is associated with increased EZH2 recruitment and increased H3K27me3, which is also seen in cells with acquired loss of hormone response (C4-12 and LTED). In these cells, chromatin is still marked by H3K4me3, thus reflecting a status of bivalent modification. DNA methylation can be observed, but it is less pronounced compared to MDA-MB-231 cells, which are fully methylated, thereby potentially decreasing the need for repressive histone modifications (depicted in a model in Fig 3I).

### **Loss of HOXC10 increases cell growth, decreases apoptosis, and enhances cell motility**

To determine if the loss of HOXC10 is causatively involved in resistance to estrogen deprivation, we generated MCF-7 pooled clones with decreased (75–80%) HOXC10 expression using two independent shRNAs (Fig 4A; table S3). MCF-7 cells with HOXC10 knockdown (sh-H1, sh-H2) grew significantly better ( $p < 0.001$ ) compared to control cells with non-silencing shRNA control (sh-ns), both in the presence and absence of estrogen (Fig 4B; table S3). This increased growth rate was associated with increased Cyclin D1 levels (insert in Fig 4B, right panel). Similar effects were observed in a second breast cancer cell line model (ZR75B). Transient knockdown of HOXC10 in ZR75B cells resulted in increased proliferation of the cells in charcoal stripped serum (CSS) as well as in serum-free medium (SFM), but not in full serum (Fig 4C; table S3). This was, however, not generalizable to all resistant models, as transient knockdown of HOXC10 had no effect in MDA-MB-361 cells and resulted in a decrease of growth in T47D cells (Fig S6). MCF-7 cells with HOXC10 knockdown also showed increased anchorage-independent growth, both in the presence and absence of estrogen (Fig 4D; table S3). We also observed increased anchorage-dependent and anchorage-independent growth of the HOXC10 knockdown clones in the presence of tamoxifen, suggesting that HOXC10 might have a role in tamoxifen resistance (Fig S7).

When studying apoptosis, we did not detect differences with E2 in 5% CSS, but there were marked differences in estrogen-deprived conditions (Fig 4E; table S3). In contrast to sh-ns control cells, sh-H1 cells completely lacked induction of apoptosis, and apoptosis was decreased in the sh-H2 clone. This decrease in apoptosis was reflected by a reduced induction of cleaved PARP (Fig 4E, right panel). HOXC10 knockdown cells also displayed enhanced migration (Fig 4F and 4G; table S3), compared to the control. In summary, loss of HOXC10 caused MCF-7 cells to become more aggressive and less sensitive to estrogen deprivation therapy, as reflected by increased growth in 2D and in 3D cultures, increased motility and migration, and reduced apoptosis.

### **Loss of HOXC10 promotes resistance to estrogen deprivation *in vivo***

To determine if HOXC10 plays a role in endocrine resistance *in vivo* we used an endocrine resistance xenograft model. MCF-7 cells were grown in estrogen-supplemented mice, and then randomized to receive continued estrogen supplementation or estrogen deprivation (Fig 5A; table S3). As expected, removal of estrogen slowed growth; however, tumors soon acquired resistance to estrogen deprivation and continued to grow. Consistent with our *in vitro* data, HOXC10 levels were significantly lower in the xenografts resistant to estrogen deprivation compared to the estrogen-stimulated xenografts ( $p = 0.0069$ ) (Fig 5B; table S3).



To directly examine the effect of HOXC10 knockdown on endocrine sensitivity *in vivo*, we performed an experiment similar to Fig 5A, but injected MCF-7 control and HOXC10 knockdown cells. In the sh-ns clone, removal of the estrogen pellet resulted in rapid shrinkage of all tumors with the exception of one outlier (Fig 5C, left panels; table S3). In contrast, the majority of sh-H1 tumors continued to grow when estrogen was removed. Because the tumors in this model did not follow a homogenous growth rate, we analyzed the tumor growth using a previously described piecewise linear (“broken stick”) model (23) (Fig 5C, right panel; table S3), which clearly indicated that clone sh-H1 was resistant to estrogen deprivation. A second clone (sh-H2) grew similar to the control (Fig S8A, right panel) and didn’t show down-regulation of HOXC10 levels *in vivo* (Fig S8B). qPCR analysis confirmed significant downregulation of HOXC10 *in vivo* in the sh-H1 clone ( $p=0.032$ ) (Fig S8B). To determine whether the increased growth of the HOXC10 sh-H1 clone *in vivo* was a result of decreased apoptosis and/or increased proliferation, we repeated the experiment, but tumors were harvested at an earlier time point so that material was available for *in situ* analysis. As expected, estrogen removal caused a decrease in proliferation and an increase in apoptosis, however these effects were attenuated in sh-H1 (Fig 5D; table S3). Collectively, these data suggest that loss of HOXC10 can confer resistance to estrogen deprivation *in vivo*, and the main mechanism of action is a prevention of apoptosis.

### HOXC10 levels are reduced in breast tumors which recur on AI therapy

To determine whether HOXC10 is lost in breast tumors which recur during AI therapy, we measured HOXC10 in 5 matched primary-recurrent tumor pairs (Fig 6A). We measured HOXC10 by IHC (Fig 6B) or qPCR (Fig 6C), depending upon the source of specimens (FFPE or frozen). Supporting our hypothesis, we found decreased HOXC10 in 4/5 recurrences. In the remaining pair (RCS#2), HOXC10 was already undetectable in the primary tumor. We also measured HOXC10 in 2 matched primary-recurrent tumor pairs from tamoxifen-treated patients (RCS#4 and RCS#5), and again we detected decreased HOXC10 expression in the recurrences (Fig 6B). Thus, HOXC10 levels are low in recurrences from endocrine-treated breast tumors, providing evidence for clinical relevance of our findings.

## DISCUSSION

We report that HOXC10 promoter methylation is a determinant of endocrine resistance in breast cancer. An unbiased genome-wide promoter methylation screen in long-term estrogen-deprived C4-12 and LTED cells identified widespread genomic hyper- and hypomethylation, with hypermethylation being three-fold more frequent than hypomethylation. We report HOXC10 methylation and subsequent loss of expression causing aggressive *in vitro* and *in vivo* tumor growth in the absence of estrogen, primarily mediated by loss of apoptosis. HOXC10 expression is repressed by estrogen *in vitro* and *in vivo* to promote tumor growth. Short-term estrogen withdrawal induces HOXC10 to induce growth arrest and apoptosis, but its long-term absence results in permanent repression mediated by methylation. This repression counteracts the therapeutic benefit of estrogen withdrawal.

There is increasing evidence implicating HOX genes in cancer (24). Deregulation of HOX gene expression is frequently caused by epigenetic changes, including DNA methylation (25). There is also prior evidence for a role of HOX genes in endocrine treatment response in breast cancer (26), however, these studies were performed in the setting of tamoxifen resistance, whereas our study focuses on resistance to AI.

HOXC10 encodes a transcription factor containing a conserved DNA-binding homeodomain (27). HOXC10 has also been implicated in replication, where it binds in a structure-dependent manner to origins of replication, and contributes to the assembly of replicative complexes (28, 29). Our finding of strong regulation of HOXC10 in the cytoplasm also implies a role for HOXC10 outside the nucleus. Further studies will need to focus on the mechanism of action of HOXC10 in cancer cells, to understand how HOXC10 mediates its effects on proliferation, apoptosis, and invasive phenotypes.

Intriguingly, in cervical cancer cells, HOXC10 is associated with increased invasiveness (30). We also observed high HOXC10 expression in a subset of primary tumors (as shown in our IHC studies), and knockdown of HOXC10 decreased growth of T47D cells and didn't affect growth in MDA-MB-361. A recent study by Ansari *et al* suggested estrogen induction of HOXC10 (31). The different roles for HOXC10 may depend on cell type and specific genetic background, an observation with increasing relevance in the era of "personalized" medicine. It is also possible that HOXC10 might play a role in some ER+/ER- primary tumors that is different from its role in tumors with acquired endocrine resistance. There is an increasing realization that the mechanism involved in primary resistance might be different from those involved in secondary (acquired) resistance, with the identification of ESR1 mutations being a recent example (9), and it is thus critical to model these diverse clinical observations *in vitro*.

Finally, our studies contribute to a general model of epigenetic reprogramming in endocrine resistance. Given estrogen regulation of HOX gene expression (31) and the previously reported links between ER and EZH2 (32), we analyzed the role of EZH2 and H3K27me3/H3K4me3 in the progression to AI resistance. In ES cells, polycomb proteins are recruited to the HOXC10 promoter, which displays both H3K4me3 and H3K27me3 marks (33). These 'bivalent' modifications frequently mark genes which are central to the developmental potential of ES cells and which are required to be in a "poised" state, ready to be transcriptionally regulated (34). In MCF-7 cells, the HOXC10 regulatory region contains open chromatin marked by H3K4me3, thus allowing for estrogen response. Loss of hormone response, such as in C4-12 and LTED cells, is associated with increased EZH2 recruitment and H3K27 trimethylation. ER and EZH2 may compete with each other for binding to the -1.6 kb region in the HOXC10 promoter, and loss of ER signaling then results in recruitment of EZH2. In C4-12 and LTED, the HOXC10 regulatory region contains both the H3K27me3 and H3K4me3 marks, and thus the HOXC10 promoter possesses 'bivalent' modifications similar to ES cells, suggesting a potential "dedifferentiation". Increased H3K27me3 is accompanied by increasing hypermethylation, presumably through interaction between EZH2 and DNMTs (35), resulting in "epigenetic switching". Interestingly, exposure of mammospheres to estrogen has been shown to promote a repressive mode of chromatin, followed by DNA methylation (36). Given that a number of developmental genes



were methylated in our study, our results support a model of epigenetic reprogramming during transition from undifferentiated cells to hormone responsive cells, and finally to a state characterized by hormone resistance.

Our present study has some limitations. First, the identification of methylated candidate regions was limited by the use of an Affymetrix array which contains promoters of >25,000 genes, but does not contain non-promoter regions which could be differentially methylated and important in AI resistance. Additional studies using recently developed methods, such as genome-wide bisulfite sequencing followed by systems biology analyses, will provide further insight. Second, given the relatively small sample size of the clinical specimens it is not clear how generalizable our findings are. Additional cell lines and tumors, both primary and metastatic, representing different molecular subtypes, will need to be studied to address this limitation.

Notwithstanding these shortcomings, our study clearly provides evidence that methylation of the estrogen-regulated gene HOXC10 is a causative event in resistance to estrogen deprivation, and it is likely that similar epigenetic reprogramming mechanisms will be observed for other developmental genes. Our data warrant additional studies to expand our understanding of epigenetic contributions to AI resistance in breast cancer and its therapeutic implications, with a specific emphasis on the early targeting of enzymes that mediate histone modifications. We expect that such interventions will be beneficial in blocking or delaying AI resistance.

## MATERIALS AND METHODS

### Study Design

The study was designed to identify differentially methylated genes in models of AI resistance. The mechanism of repression of a candidate gene (HOXC10) was studied in cell line models, and effects of loss of HOXC10 expression were evaluated in cell lines in vitro and in vivo. Methylation, expression, cellular proliferation in 2D and 3D, apoptosis, and signaling were monitored by methylation-specific PCR, bisulfite sequencing, standard growth assays, immunoprecipitation-based approaches, histology, qPCR, immunoblotting, and immunohistochemical methods. In vitro assays were repeated two to three times. HOXC10 expression was also studied in clinical specimens obtained from a neoadjuvant endocrine trial and from retrospective collections of matched primary and metastatic samples from breast cancer patients. Sample sizes for most studies were determined on the basis of prior knowledge or expected effect sizes, and for some analyses using clinical samples we were restricted by the availability of the specimens. For the xenograft studies, the animals were randomly assigned to the treatment groups (–/+ estrogen, and sh-ns/sh-H1/sh-H2). Full experimental details are provided below and in the Supplementary Materials.

### Cell lines

Human breast cancer cell lines from the NCI ICBP-43 panel were cultured according to ATCC instructions. C4-12 and LTED cells were maintained as previously described (12,

37). Additional longterm estrogen-deprived cells were generated through incubation of cells (ZR75B, T47D, and BT474) in CSS. Parental and estrogen-deprived MDA-MB-361 cells were kindly provided by Dr Carlos Arteaga, and have previously been described (19). Generation of HOXC10 knockdown clones is described in the Supplementary Materials and Methods.

### **GST-MBD pull-down and promoter array**

GST-MBD pull-down was performed as previously described (15) and as stated in the Supplementary Materials and Methods. Data were analyzed using Model-based Analysis of Tiling-arrays (MAT) as previously described (38). Cut offs used were  $p < 10^{-5}$  and fold change  $>2$ .

### **Xenograft studies**

Xenograft experiments were performed as previously published (39), and are detailed in the Supplementary Materials and Methods section. The animal experiments were performed according to protocols approved by the Institutional Animal Care and Use Committee at Baylor College of Medicine, Houston, TX.

### **Immunohistochemistry (IHC) and Immunofluorescence (IF)**

To measure HOXC10 after short-term AI treatment, tumors were obtained from a phase II clinical trial in which breast cancer patients were treated with exemestane alone ( $n=14$  pairs of pre and post-treatment samples), or exemestane and tamoxifen ( $n=1$ ) for 4 months, as described in Harvell et al (40). Tumor samples were obtained from pre-treatment core needle biopsies and at the final excision surgery. The protocol was approved by the Colorado Multiple Institutional Review Board (COMIRB Protocol 01-627) and informed consent was obtained from all patients prior to participation. Studies with matched primary and metastatic samples were covered by the Ethics Committee, Beaumont Hospital, Dublin (RCS samples), and by an IRB from the University of Pittsburgh (HSTB samples).

### **Statistical Analysis**

The two-sample  $t$  test was used for two-group comparisons, and unless otherwise stated, treatment groups were compared to vehicle groups. All statistical tests were two-sided. Unless otherwise indicated, “\*” in figures refers to  $p < 0.05$ , “\*\*” to  $p < 0.01$ , “\*\*\*” to  $p < 0.001$ , and “\*\*\*\*” to  $p < 0.0001$ . In vitro assays were repeated three times, and plotted values represent means  $\pm$  SD, unless otherwise stated. Descriptive statistics were generated with GraphPad Prism.

### **Supplementary Material**

Refer to Web version on PubMed Central for supplementary material.

### **Acknowledgements**

We would like to acknowledge the valuable contributions from the Frank Gannon laboratory (Drs G. Reid, H. Brand, S. Denger, and S. Johnsonat) at EMBL, especially with respect to technical details of the MBD-PD. We would also like to thank the Genomics Core at EMBL for their critical contribution to the project. Technical support

was provided by the Proteomics and Flow Cytometry Cores at the Dan L Duncan Cancer Center at BCM, and the Biostatistics Core Facility at UPCI, especially by Dr. D Normolle and K Cooper. We would also like to acknowledge support from Dr L Malorni (BCM), Mrs E Harrington (UPCI), N Spoelstra at the University of Colorado for IHC, and Dr C Arteaga for providing cell line models of resistance to estrogen deprivation. Finally, we would like to thank Dr. J Chang (Methodist Hospital Research Institute, Houston, TX) for her mentorship of Dr Pathiraja throughout her thesis project, especially with respect to understanding the clinical relevance of her studies.

#### Funding:

This project was in part funded through an Alexander von Humboldt Foundation fellowship (SO), a DOD predoctoral fellowship DOD 5W81XWH-06-1-0713 (T.N. Pathiraja), National Institutes of Health P30CA125123 (RS), P30CA47904 (ND), P50CA58183 (RS) P01CA030195 (SO), R01HG007538 (WL), R01CA94118 (AVL) and R01CA097213 (SO), Susan G. Komen for the Cure Foundation (PG12221410) to RS, the EIF/Lee Jeans Breast Cancer Research Program (RS), SU2C/ Breast Cancer Program (RS, ND), Breast Cancer Research Foundation (RS, ND, AVL, and SO), and a grant from the Pennsylvania Department of Health (SO, AVL). The Department specifically disclaims responsibility for any analyses, interpretations or conclusions.

## References and notes

1. Musgrove EA, Sutherland RL. Biological determinants of endocrine resistance in breast cancer. *Nat Rev Cancer*. 2009; 9:631–643. [PubMed: 19701242]
2. Lonning PE, Eikesdal HP. Aromatase inhibition 2013: clinical state of the art and questions that remain to be solved. *Endocrine-related cancer*. 2013; 20:R183–R201. [PubMed: 23625614]
3. Miller WR, Larionov AA. Understanding the mechanisms of aromatase inhibitor resistance. *Breast Cancer Res*. 2012; 14:201. [PubMed: 22277572]
4. Osborne CK, Schiff R. Mechanisms of endocrine resistance in breast cancer. *Annu Rev Med*. 2011; 62:233–247. [PubMed: 20887199]
5. Baselga J, Campone M, Piccart M, Burris HA 3rd, Rugo HS, Sahmoud T, Noguchi S, Gnant M, Pritchard KI, Lebrun F, Beck JT, Ito Y, Yardley D, Deleu I, Perez A, Bachelot T, Vittori L, Xu Z, Mukhopadhyay P, Lebwohl D, Hortobagyi GN. Everolimus in postmenopausal hormone-receptor-positive advanced breast cancer. *N Engl J Med*. 2012; 366:520–529. [PubMed: 22149876]
6. Jordan VC, O'Malley BW. Selective estrogen-receptor modulators and antihormonal resistance in breast cancer. *J Clin Oncol*. 2007; 25:5815–5824. [PubMed: 17893378]
7. Bautista S, Valles H, Walker RL, Anzick S, Zeillinger R, Meltzer P, Theillet C. In breast cancer, amplification of the steroid receptor coactivator gene AIB1 is correlated with estrogen and progesterone receptor positivity. *Clin Cancer Res*. 1998; 4:2925–2929. [PubMed: 9865902]
8. Slamon DJ, Clark GM, Wong SG, Levin WJ, Ullrich A, McGuire WL. Human breast cancer: correlation of relapse and survival with amplification of the HER-2/neu oncogene. *Science*. 1987; 235:177–182. [PubMed: 3798106]
9. Oesterreich S, Davidson NE. The search for ESR1 mutations in breast cancer. *Nat Genet*. 2013; 45:1415–1416. [PubMed: 24270445]
10. Huang Y, Nayak S, Jankowitz R, Davidson NE, Oesterreich S. Epigenetics in breast cancer: what's new? *Breast Cancer Res*. 2011; 13:225. [PubMed: 22078060]
11. Jansen MP, Knijnenburg T, Reijm EA, Simon I, Kerkhoven R, Droog M, Velds A, van Laere S, Dirix L, Alexi X, Foekens JA, Wessels L, Linn SC, Berns EM, Zwart W. Hallmarks of aromatase inhibitor drug resistance revealed by epigenetic profiling in breast cancer. *Cancer Res*. 2013; 73:6632–6641. [PubMed: 24242068]
12. Oesterreich S, Zhang P, Guler RL, Sun X, Curran EM, Welshons WV, Osborne CK, Lee AV. Re-expression of estrogen receptor alpha in estrogen receptor alpha-negative MCF-7 cells restores both estrogen and insulin-like growth factor-mediated signaling and growth. *Cancer Res*. 2001; 61:5771–5777. [PubMed: 11479214]
13. Jeng MH, Shupnik MA, Bender TP, Westin EH, Bandyopadhyay D, Kumar R, Masamura S, Santen RJ. Estrogen receptor expression and function in long-term estrogen-deprived human breast cancer cells. *Endocrinology*. 1998; 139:4164–4174. [PubMed: 9751496]
14. Foroni C, Broggin M, Generali D, Damia G. Epithelial-mesenchymal transition and breast cancer: role, molecular mechanisms and clinical impact. *Cancer treatment reviews*. 2012; 38:689–697. [PubMed: 22118888]

15. Kangaspeska S, Stride B, Metivier R, Polycarpou-Schwarz M, Ibberson D, Carmouche RP, Benes V, Gannon F, Reid G. Transient cyclical methylation of promoter DNA. *Nature*. 2008; 452:112–115. [PubMed: 18322535]
16. Pollard SM, Stricker SH, Beck S. Preview. A shore sign of reprogramming. *Cell Stem Cell*. 2009; 5:571–572. [PubMed: 19951682]
17. Irizarry RA, Ladd-Acosta C, Wen B, Wu Z, Montano C, Onyango P, Cui H, Gabo K, Rongione M, Webster M, Ji H, Potash JB, Sabunciyan S, Feinberg AP. The human colon cancer methylome shows similar hypo- and hypermethylation at conserved tissue-specific CpG island shores. *Nat Genet*. 2009; 41:178–186. [PubMed: 19151715]
18. Krum SA, Miranda-Carboni GA, Lupien M, Eeckhoute J, Carroll JS, Brown M. Unique ERalpha cistromes control cell type-specific gene regulation. *Mol Endocrinol*. 2008; 22:2393–2406. [PubMed: 18818283]
19. Miller TW, Balko JM, Fox EM, Ghazoui Z, Dunbier A, Anderson H, Dowsett M, Jiang A, Smith RA, Maira SM, Manning HC, Gonzalez-Angulo AM, Mills GB, Higham C, Chanthaphaychith S, Kuba MG, Miller WR, Shyr Y, Arteaga CL. ERalpha-dependent E2F transcription can mediate resistance to estrogen deprivation in human breast cancer. *Cancer Discov*. 2011; 1:338–351. [PubMed: 22049316]
20. Rea S, Eisenhaber F, O'Carroll D, Strahl BD, Sun ZW, Schmid M, Opravil S, Mechtler K, Ponting CP, Allis CD, Jenuwein T. Regulation of chromatin structure by site-specific histone H3 methyltransferases. *Nature*. 2000; 406:593–599. [PubMed: 10949293]
21. Atkinson SP, Koch CM, Clelland GK, Willcox S, Fowler JC, Stewart R, Lako M, Dunham I, Armstrong L. Epigenetic marking prepares the human HOXA cluster for activation during differentiation of pluripotent cells. *Stem Cells*. 2008; 26:1174–1185. [PubMed: 18292213]
22. Bernstein BE, Mikkelsen TS, Xie X, Kamal M, Huebert DJ, Cuff J, Fry B, Meissner A, Wernig M, Plath K, Jaenisch R, Wagschal A, Feil R, Schreiber SL, Lander ES. A bivalent chromatin structure marks key developmental genes in embryonic stem cells. *Cell*. 2006; 125:315–326. [PubMed: 16630819]
23. Zhao L, Morgan MA, Parsels LA, Maybaum J, Lawrence TS, Normolle D. Bayesian hierarchical changepoint methods in modeling the tumor growth profiles in xenograft experiments. *Clin Cancer Res*. 2011; 17:1057–1064. [PubMed: 21131555]
24. Abate-Shen C. Deregulated homeobox gene expression in cancer: cause or consequence? *Nat Rev Cancer*. 2002; 2:777–785. [PubMed: 12360280]
25. Fackler MJ, Umbricht CB, Williams D, Argani P, Cruz LA, Merino VF, Teo WW, Zhang Z, Huang P, Visvanathan K, Marks J, Ethier S, Gray JW, Wolff AC, Cope LM, Sukumar S. Genome-wide methylation analysis identifies genes specific to breast cancer hormone receptor status and risk of recurrence. *Cancer Res*. 2011; 71:6195–6207. [PubMed: 21825015]
26. Shah N, Jin K, Cruz LA, Park S, Sadik H, Cho S, Goswami CP, Nakshatri H, Gupta R, Chang HY, Zhang Z, Cimino-Mathews A, Cope L, Umbricht C, Sukumar S. HOXB13 mediates tamoxifen resistance and invasiveness in human breast cancer by suppressing ERalpha and inducing IL-6 expression. *Cancer Res*. 2013; 73:5449–5458. [PubMed: 23832664]
27. Shah N, Sukumar S. The Hox genes and their roles in oncogenesis. *Nat Rev Cancer*. 10:361–371. [PubMed: 20357775]
28. Falaschi A, Abdurashidova G, Biamonti G. DNA replication, development and cancer: a homeotic connection? *Crit Rev Biochem Mol Biol*. 2010; 45:14–22. [PubMed: 19919294]
29. Marchetti L, Comelli L, D'Innocenzo B, Puzzi L, Luin S, Arosio D, Calvello M, Mendoza-Maldonado R, Peverali F, Trovato F, Riva S, Biamonti G, Abdurashidova G, Beltram F, Falaschi A. Homeotic proteins participate in the function of human-DNA replication origins. *Nucleic Acids Res*. 2010; 38:8105–8119. [PubMed: 20693533]
30. Zhai Y, Kuick R, Nan B, Ota I, Weiss SJ, Trimble CL, Fearon ER, Cho KR. Gene expression analysis of preinvasive and invasive cervical squamous cell carcinomas identifies HOXC10 as a key mediator of invasion. *Cancer Res*. 2007; 67:10163–10172. [PubMed: 17974957]
31. Ansari KI, Hussain I, Kasiri S, Mandal SS. HOXC10 is overexpressed in breast cancer and transcriptionally regulated by estrogen via involvement of histone methylases MLL3 and MLL4. *J Mol Endocrinol*. 2012; 48:61–75. [PubMed: 22143955]

32. Shi B, Liang J, Yang X, Wang Y, Zhao Y, Wu H, Sun L, Zhang Y, Chen Y, Li R, Hong M, Shang Y. Integration of estrogen and Wnt signaling circuits by the polycomb group protein EZH2 in breast cancer cells. *Mol Cell Biol.* 2007; 27:5105–5119. [PubMed: 17502350]
33. Vastenhouw NL, Schier AF. Bivalent histone modifications in early embryogenesis. *Current opinion in cell biology.* 2012; 24:374–386. [PubMed: 22513113]
34. Pan G, Tian S, Nie J, Yang C, Ruotti V, Wei H, Jonsdottir GA, Stewart R, Thomson JA. Whole-genome analysis of histone H3 lysine 4 and lysine 27 methylation in human embryonic stem cells. *Cell Stem Cell.* 2007; 1:299–312. [PubMed: 18371364]
35. Vire E, Brenner C, Deplus R, Blanchon L, Fraga M, Didelot C, Morey L, Van Eynde A, Bernard D, Vanderwinden JM, Bollen M, Esteller M, Di Croce L, de Launoit Y, Fuks F. The Polycomb group protein EZH2 directly controls DNA methylation. *Nature.* 2006; 439:871–874. [PubMed: 16357870]
36. Cheng AS, Culhane AC, Chan MW, Venkataramu CR, Ehrich M, Nasir A, Rodriguez BA, Liu J, Yan PS, Quackenbush J, Nephew KP, Yeatman TJ, Huang TH. Epithelial progeny of estrogen-exposed breast progenitor cells display a cancer-like methylome. *Cancer Res.* 2008; 68:1786–1796. [PubMed: 18339859]
37. Yue W, Wang JP, Conaway M, Masamura S, Li Y, Santen RJ. Activation of the MAPK pathway enhances sensitivity of MCF-7 breast cancer cells to the mitogenic effect of estradiol. *Endocrinology.* 2002; 143:3221–3229. [PubMed: 12193533]
38. Johnson WE, Li W, Meyer CA, Gottardo R, Carroll JS, Brown M, Liu XS. Model-based analysis of tiling-arrays for ChIP-chip. *Proc Natl Acad Sci U S A.* 2006; 103:12457–12462. [PubMed: 16895995]
39. Massarweh S, Osborne CK, Jiang S, Wakeling AE, Rimawi M, Mohsin SK, Hilsenbeck S, Schiff R. Mechanisms of tumor regression and resistance to estrogen deprivation and fulvestrant in a model of estrogen receptor-positive, HER-2/neu-positive breast cancer. *Cancer Res.* 2006; 66:8266–8273. [PubMed: 16912207]
40. Harvell DM, Spoelstra NS, Singh M, McManaman JL, Finlayson C, Phang T, Trapp S, Hunter L, Dye WW, Borges VF, Elias A, Horwitz KB, Richer JK. Molecular signatures of neoadjuvant endocrine therapy for breast cancer: characteristics of response or intrinsic resistance. *Breast cancer research and treatment.* 2008; 112:475–488. [PubMed: 18327671]

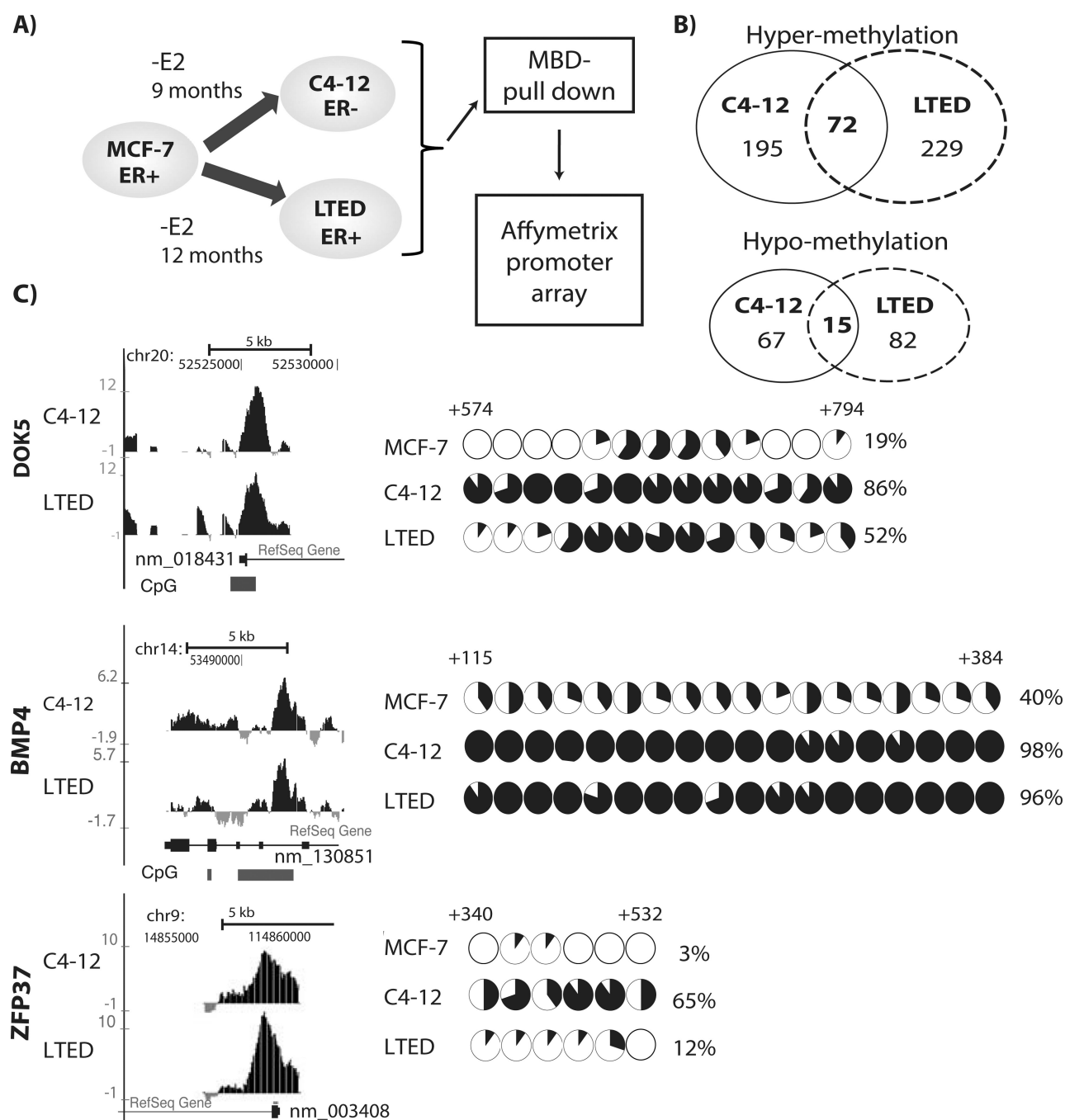


**Figure 1. Frequent hypo- and hyper-methylation in breast cancer cells resistant to estrogen deprivation**

A) Schematic representation of cell line models resistant to estrogen deprivation used in this study, and genome-wide methylation analysis.

B) Venn diagrams showing overlap of hypermethylated and hypomethylated genes in C4-12 (solid line) and LTED (dashed line).

C) Confirmation of candidate hypermethylated genes identified by MBD-PD array.

Methylation tracks for C4-12 and LTED compared to MCF-7 viewed on the UCSC genome



browser ([www.http://genome.ucsc.edu/](http://genome.ucsc.edu/)) (hg18) (left). The NCBI reference sequence IDs are indicated in the tracks. The y-axis represents fold methylation relative to MCF-7, and upward and downward peaks represent hypermethylated and hypomethylated regions, respectively. Corresponding results of the bisulfite sequencing (BS) assay in MCF-7, C4-12 and LTED cells are shown on the right. Each CpG site is represented by a circle and mean % methylation at each CpG site is shown by the fraction of dark shading inside.

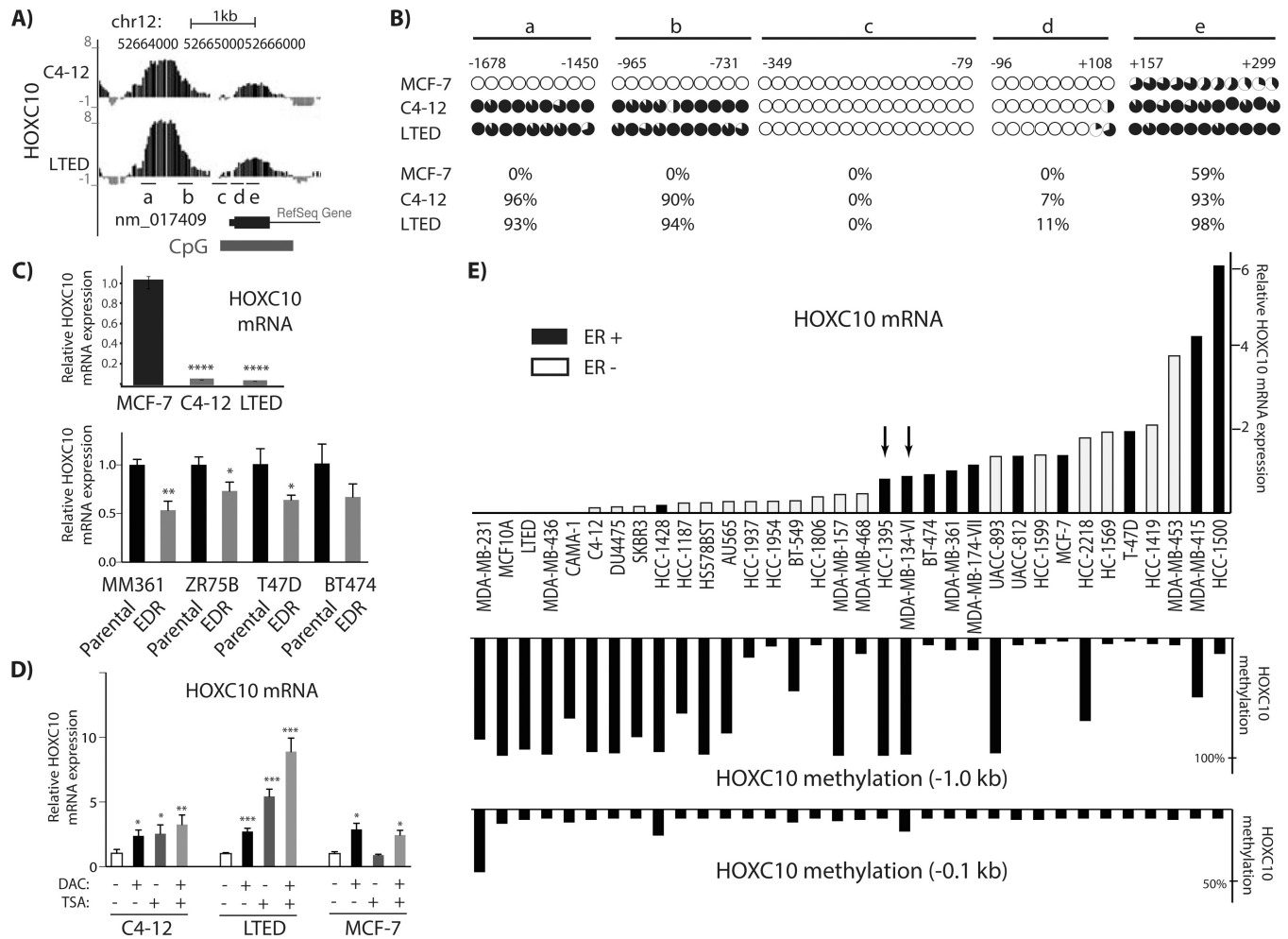


### Figure 2. Methylation and expression of HOXC10 in breast cancer cells

A) UCSC genome browser figure showing hypermethylated *HOXC10* regions in C4-12 and LTED cells. Methylation tracks are shown as described in Fig 1C. The locations of BS primers are depicted as lines labeled a, b, c, d and e.

B) *Bisulfite sequencing at an upstream promoter region/CpG shore (a and b), proximal promoter (c and d) and first exon (e) in HOXC10.* Each CpG site is represented by a circle and mean % methylation at each CpG site is shown by the fraction of dark shading.

C) *Relative mRNA expression of HOXC10 in cells resistant to estrogen deprivation.* Relative amount of mRNA is depicted as fold change compared to MCF-7 (top panel) (mean  $\pm$  SD). HOXC10 mRNA levels were determined in other ER+ parental cell lines and clones resistant to estrogen deprivation (“EDR”) (bottom panel). \* $p < 0.05$ , \*\* $p < 0.01$ , (t-test compared to respective parental cells). Exact p-values are provided in Table S4.

D) *Effect of DAC and TSA treatment on HOXC10 expression.* q-RT-PCR was used to determine the relative HOXC10 mRNA expression after C4-12, LTED, and MCF-7 cells were treated with DAC for 6 days and TSA for 14 hours. Data are mean  $\pm$  SD from 3 biological replicates, and presented as fold over vehicle control. \* $p < 0.05$ , \*\* $p < 0.01$ , \*\*\* $p < 0.001$  (t-test compared to vehicle treated cells). Exact p-values are provided in Table S4.

E) *HOXC10* methylation inversely correlates with gene expression in breast cancer cell lines. q-RT-PCR and bisulfite pyrosequencing were used to quantify expression of *HOXC10* and promoter methylation, respectively, in 34 breast cancer cell lines. ER status of the cell lines is shown by black (ER+) and white (ER–) boxes. The relative mRNA level is depicted as fold change compared to the average set as 1.

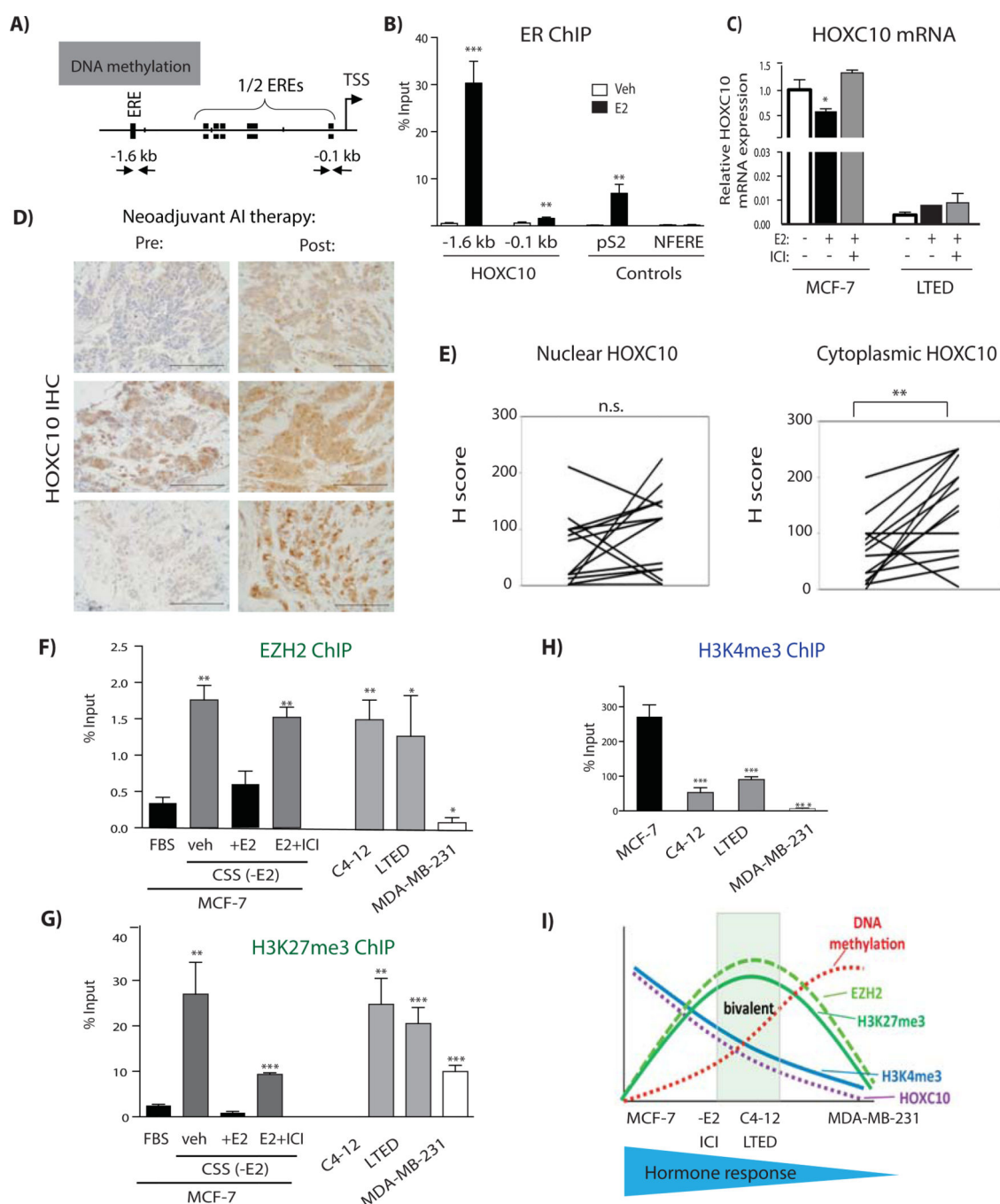


**Figure 3. Estrogen regulation of HOXC10 expression, and histone marks in HOXC10 promoter**

A) Model showing ERE sites in *HOXC10* promoter and position of primers used in ChIP assays. Hypermethylated CpG shore region is shown by a shaded box.

B) ER ChIP assays in MCF-7 cells. Cells were treated with vehicle or E2 (45 min), and ER recruitment to different positions in the *HOXC10* promoter, pS2 (positive control), and NFERE (negative control) was determined. Bars represent mean  $\pm$  SD from three biological replicates. \*\*p < 0.01, \*\*\*p < 0.001 (t-test comparing vehicle and E2 treated cells). Exact p-values are provided in Table S4.

C) *Estrogen-mediated repression of HOXC10*. The relative mRNA expression, measured by q-RT-PCR, is depicted as ligand-mediated fold change compared to vehicle (ethanol). Cells were treated for 16 hours with either vehicle, E2, or E2 and ICI 172,780.  $P=0.0236$  (t-test compared to vehicle treated cells).

D) *HOXC10 protein expression in clinical breast cancer specimens*. Representative samples of HOXC10 IHC in ER+ tumors acquired before (pre) and after (post) neoadjuvant AI therapy. Scale bars represent 100  $\mu\text{m}$ .

E) *Quantification of HOXC10 protein expression in clinical breast cancer specimens*. Graphical presentation of nuclear and cytoplasmic H scores.  $P=0.003$  (paired t-test).

F) *EZH2 recruitment at the HOXC10 –1.6 kb site after short-term and long-term E2 deprivation*. EZH2 and H3K27me3 ChIP assays in MCF7 cells after culturing in FBS or in CSS (3 days) followed by treatment with veh, E2, or E2 and ICI (45 min). Bars represent mean  $\pm$  SD from three biological replicates.  $*p < 0.05$ ,  $**p < 0.01$  (left panel: t-test compared to vehicle treated cells; right panel: t-test compared to MCF-7). Exact p-values are provided in Table S4.

G) *H3K27me3 marks at the HOXC10 –1.6 kb site after short-term and long-term E2 deprivation*. Treatments in ChIP studies were performed and analyzed as in Fig 3F.  $**p < 0.01$ ,  $***p < 0.001$ . Exact p-values are provided in Table S4.

H) *H3K4me3 marks at the HOXC10 –1.6 kb site*. ChIP assays were performed and analyzed as in Fig 3F.  $***p < 0.001$ . Exact p-values are provided in Table S4.

I) *Model for associations between ER activity, HOXC10 expression, promoter methylation, and histone marks*. The central grey square (“bivalent”) marks a state in which the cells have both active H3K4me3 and repressive H3K27me3.

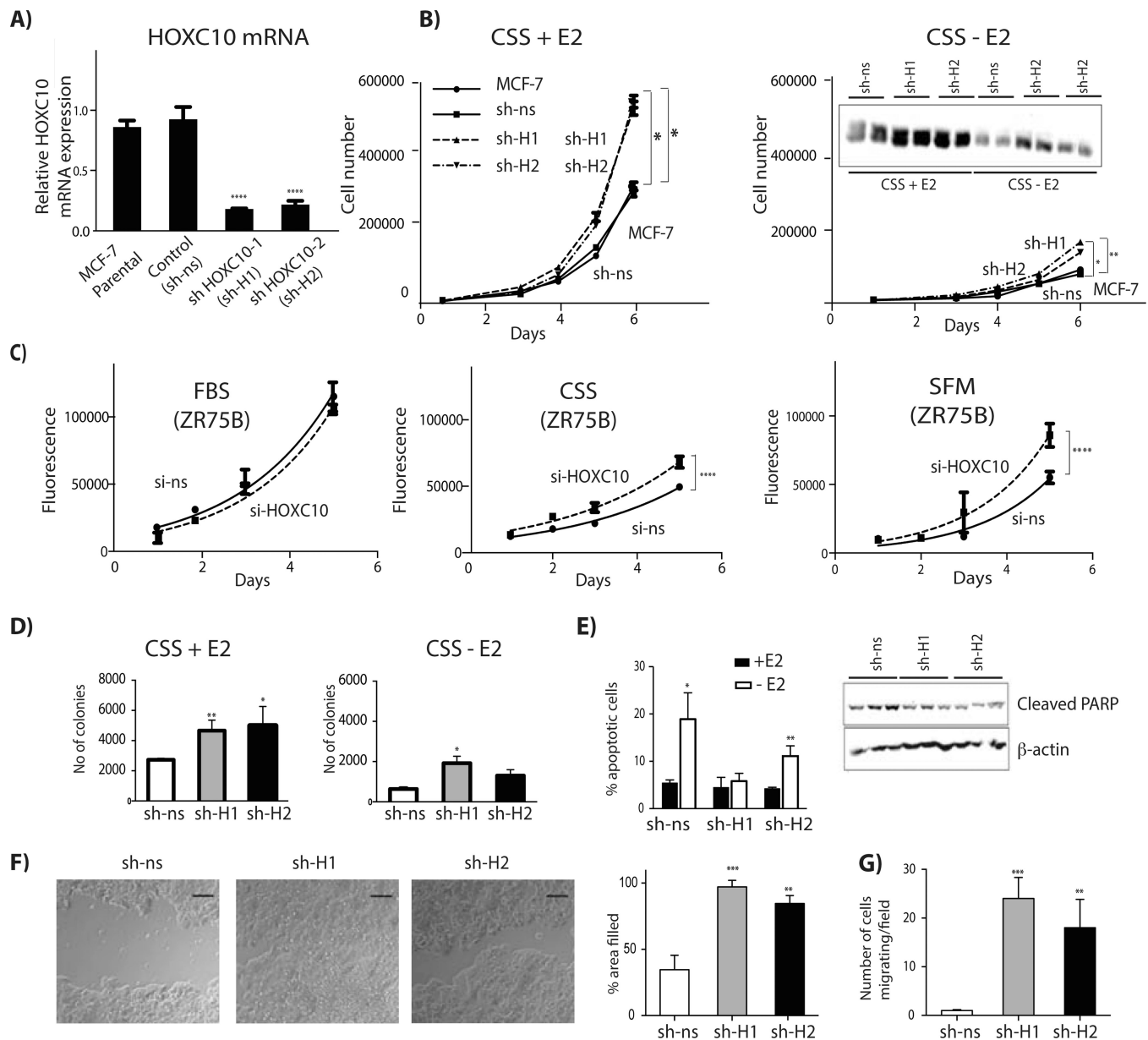


**Figure 4. Effect of HOXC10 loss on cell growth, apoptosis, and cell motility**

**A) ShRNA-mediated knockdown of HOXC10 expression.** HOXC10 expression was analyzed by q-RT-PCR in MCF-7 parental, control (sh-ns), and HOXC10 knockdown (sh-H1 and sh-H2) cells. Data are mean  $\pm$  SD from three biological replicates. \*\*\* $p < 0.001$  (t-test compared to sh-ns). Exact p-values are provided in Table S4.

**B) HOXC10 knockdown increases cell proliferation.** Growth curves are shown for MCF-7, sh-ns, sh-H1, and sh-H2 cells in CSS +  $10^{-8}$ M E2, or CSS + veh (-E2). The data are mean  $\pm$  SEM from three biological replicates. \* $p < 0.05$ , \*\* $p < 0.01$  (regression analysis comparing sh-H1 or sh-H2 to sh-ns). Exact p-values are provided in Table S4. The insert shows a cyclin D1 IB from parallel cultures.

**C) HOXC10 knockdown increases proliferation in ZR75B cells.** Growth curve after transient transfection with scramble siRNA (si-ns) or with HOXC10 siRNA and incubation in FBS,



or CSS, or SFM. Data are mean  $\pm$  SEM from seven biological replicates. \*\*\*\* $p < 0.001$  (regression analysis). Exact p-values are provided in Table S4.

D) *HOXC10 knockdown stimulates anchorage-independent growth*. Sh-ns, sh-H1, and sh-H2 cells were plated in soft agar with CSS in the presence ( $10^{-8}$ M) or absence of E2. The data are mean  $\pm$  SD, from three biological replicates. \* $p < 0.05$ , \*\* $p < 0.01$  (t-test). Exact p-values are provided in Table S3.

E) *ShRNA-mediated knockdown of HOXC10 reduces apoptosis*. Sh-ns, sh-H1, and sh-H2 cells were cultured in CSS in the presence or absence of vehicle or  $10^{-8}$ M E2 for 4 days, followed by measurement of apoptosis using Annexin V binding assay. The data are means  $\pm$  SD, from three biological replicates. The right panel shows IB for cleaved PARP (and  $\beta$ -actin as loading control) using the indicated lysates at 0, 3 hours, and 6 hours after switching to CSS (-E2).

F) *ShRNA-mediated knockdown of HOXC10 enhances cell motility*. Sh-ns, sh-H1, and sh-H2 were seeded at the same density, scratched, and photographed 72 hours later. Scale bar is 50  $\mu$ m. The data are means  $\pm$  SD, from three biological replicates. \*\* $p < 0.01$ , \*\*\* $p < 0.001$ . Exact p-values are provided in Table S4.

G) *ShRNA-mediated knockdown of HOXC10 enhances cell migration*. Migration assays were performed in Boyden chambers with 5% serum as chemo-attractant. Migrating cells were counted in three different fields, and three biological replicates were used to calculate means  $\pm$  SD. \*\* $p < 0.01$ , \*\*\* $p < 0.001$ . Exact p-values are provided in Table S4.

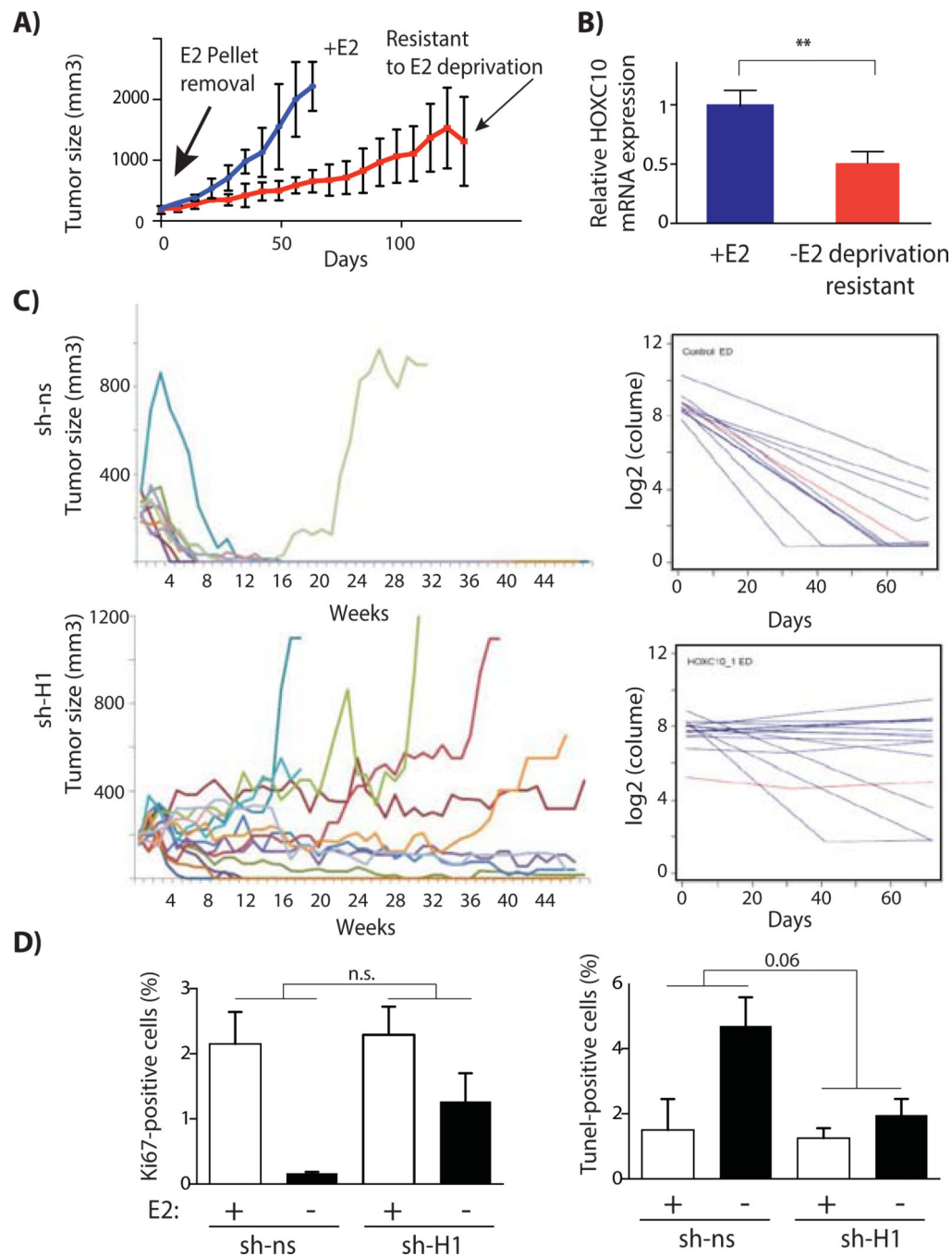


**Figure 5. Effect of HOXC10 knockdown on endocrine resistance in breast tumor xenografts**

**A) Growth of MCF-7 xenografts.** Ovariectomized athymic nude mice bearing tumors derived from MCF7 cells were randomly assigned to +E2 (continued estrogen supplementation via E2 pellet), or to -E2, estrogen deprivation (removal of E2 pellet). This resulted in growth retardation, followed by outgrowth of resistant clone(s). The data are means  $\pm$  SD of tumor growth from three independent mice in each group.

**B) HOXC10 mRNA is downregulated in endocrine-resistant xenografts.** q-RT-PCR was used to quantify HOXC10 mRNA in +E2 tumors and -E2 resistant tumors (from experiment

shown in Fig 5A). The relative mRNA expression is depicted as fold change compared to +E2 group and represents means  $\pm$  SD (N=3 mice per group). P = 0.0069 (t-test).

C) *Downregulation of HOXC10 causes resistance to estrogen deprivation.* Sh-ns (n=10) and sh-H1 (n=13) cells were injected into nude mice, E2 pellet was removed when tumors reached 150–200 mm<sup>3</sup>, and tumor volume was measured over time. Right panel: Comparisons of estimated animal profiles (blue) to estimated population profile (red) for sh-ns and sh-H1 clone. For this analysis, we used the piecewise linear model for each animal's log-transformed tumor volume over time (23).

D) *Increased proliferation and decreased apoptosis in HOXC10 knockdown xenograft.*

Tumors from shns and sh-H1 clones grown for 3 weeks in the presence or absence of E2 were harvested and stained by IHC for Ki67 (n=6–9) and TUNEL (n=3–6) to determine effects on proliferation and apoptosis, respectively. Two-way ANOVA was used to compare effects on proliferation and apoptosis between sh-ns and sh-H1.

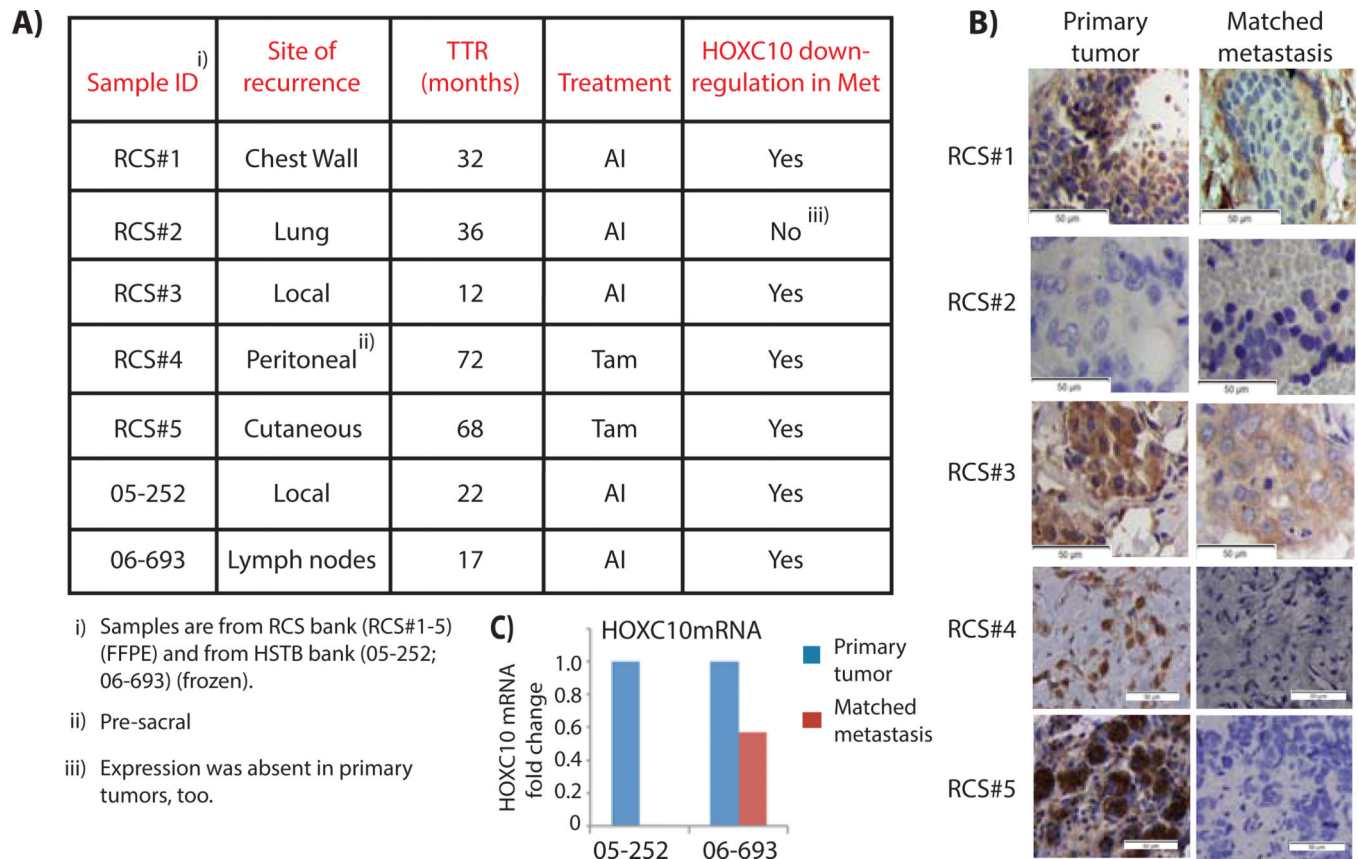


**Figure 6. HOXC10 expression in breast tumor recurrences from AI-treated patients**

A) Clinical information about recurrent tumors. TTR=time to recurrence.

B) HOXC10 protein expression in matched primary and recurrent tumors. FFPE samples from primary tumors and recurrences in chest wall, lung, and breast were stained for HOXC10 by IHC. Scale bar is 50  $\mu$ m.

C) HOXC10 RNA expression in matched primary and recurrent tumors. HOXC10 was measured by qPCR in primary tumors and matched recurrences, and data are presented relative to the levels in the primary tumor. N=1 for each sample.